Contrib Mineral Petrol (2014) 168:1052
DOI 10.1007/s00410-014-1052-0

ORIGINAL PAPER

The role of eclogite in the mantle heterogeneity at Cape Verde

A. K. Barker · P. M. Holm · V. R. Troll

Received: 24 March 2014 / Accepted: 5 August 2014 / Published online: 27 August 2014

Abstract The Cape Verde hotspot, like many other Ocean Island Basalt provinces, demonstrates isotopic heterogeneity on a 100–200 km scale. The heterogeneity is represented by the appearance of an EM1-like component at several of the southern islands and with a HIMU-like component present throughout the archipelago. Where the EM1-like component is absent, a local DMM-like component replaces the EM1-like component. Various source lithologies, including peridotite, pyroxenite and eclogite have been suggested to contribute to generation of these heterogeneities; however, attempts to quantify such contributions have been limited. We apply the minor elements in olivine approach (Sobolev et al. in Nature 434:590–597, 2005; Science, doi:10.1126/science.1138113, 2007), to determine and quantify the contributions of peridotite, pyroxenite and eclogite melts to the mantle heterogeneity observed at Cape Verde. Cores of olivine phenocrysts of the Cape Verde volcanics have low Mn/FeO and low Ni*FeO/MgO that deviate from the negative trend of the global array. The global array is defined by mixing between peridotite and pyroxenite, whereas the Cape Verde volcanics indicate contribution of an additional eclogite source. Eclogite melts escape reaction with peridotite either by efficient extraction in an area of poor mantle flow or by reaction of eclogite melts with peridotite, whereby an abundance of eclogite can seal off the melt from further reaction. Temporal trends of decreasing Mn/FeO indicate that the supply of eclogite melts is increasing. Modelling suggests the local DMM-like end-member is formed from a relatively peridotite-rich melt, while the EM1-like end-member has a closer affinity to a mixed peridotite–pyroxenite–eclogite melt. Notably the HIMU-like component ranges from pyroxenite–peridotite-rich melt to one with up to 77 % eclogite melt as a function of time, implying that sealing of melt pathways is becoming more effective.

Keywords Ocean Island Basalt · Olivine · Peridotite · Pyroxenite · Eclogite · Cape Verde

Communicated by J. Hoefs.

Electronic supplementary material The online version of this article (doi:10.1007/s00410-014-1052-0) contains supplementary material, which is available to authorized users.

A. K. Barker (✉) · V. R. Troll
CEMPEG, Department of Earth Sciences, Uppsala University, Villavägen 16, 752 36 Uppsala, Sweden
e-mail: Abigail.Barker@geo.uu.se

P. M. Holm
Department of Geosciences and Natural Resource Management, University of Copenhagen, Øster Voldgade 10, 1350 Copenhagen, Denmark

Introduction

Ocean Island Basalts (OIB) are commonly used as proxies for mantle geochemistry. OIBs tend to be more heterogeneous than mid-ocean ridge basalts (MORB), with individual Ocean Island groups displaying significant isotopic heterogeneity (e.g. Geist et al. 1988; Gerlach et al. 1988; Hoernle et al. 2000; Eisele et al. 2003; Regelous et al. 2003; Thirlwall et al. 2004; Abouchami et al. 2005). Isotopic heterogeneity has been classified according to a host of end-members and mixtures thereof, the most frequently referred to are HIMU, DMM, EM1 and EM2 (Hart 1984; Zindler and Hart 1986; Stracke et al. 2005). These mantle end-members have a variety of possible origins including (a) recycled ocean crust and sediments sampled by mantle plumes, (b) subcontinental lithospheric mantle or (c)

lower crust sampled through delamination, rifting and edge driven convection (e.g. Hoernle et al. 1991; Kokfelt et al. 1998; Doucelance et al. 2003; Escrig et al. 2005; Abratis et al. 2002; Geldmacher et al. 2008; Martins et al. 2009; Barker et al. 2010; Gurenko et al. 2010a).

Recycling of ocean crust through subduction zones is expected not only to introduce heterogeneity into the mantle, but will transform the subducted materials into eclogite at high pressures, thus introducing geochemical diversity into the mantle that will influence subsequent melting dynamics (e.g. Kogiso et al. 2003, 2004a). This concept has led to an interest in determining the source lithologies that correspond to the observed isotopic heterogeneities. One approach has been to compare bulk geochemistry of Ocean Island Basalts with the compositions of experimentally derived melts (e.g. Hirose and Kushiro 1993; Hirschmann et al. 2003; Dasgupta et al. 2006, 2007; Prytulak and Elliott 2007). Another approach is based on minor element compositions, such as Mn and Ni in olivine, and aims to distinguish between peridotite and pyroxenite source lithologies (Sobolev et al. 2005, 2007; Gurenko et al. 2009, 2010a).

Here, we adopt the minor elements in olivine approach to characterise the source lithologies associated with the isotope heterogeneity at Cape Verde (Gerlach et al. 1988; Doucelance et al. 2003; Holm et al. 2006; Barker et al. 2010). We use this method to quantify the affinity of magmas associated with the HIMU-like, local DMM-like and EM1-like end-members observed. We then consider the implications for the origin of mantle source heterogeneity at Cape Verde.

Approach

Eclogite lithologies are more fertile than peridotite, and thus, they begin to melt deeper in the mantle (e.g. Yaxley and Green 1998). These early eclogite-derived melts react with peridotite to form hybrid pyroxenite. The resulting olivine-free pyroxenite later melts to produce Ni-rich melts releasing the incompatible Ni inherited by the pyroxenite from the peridotite (Sobolev et al. 2005, 2007; Herzberg 2011). Additionally, the pyroxenite melts are low in Mn due to retention of Mn by garnet. Olivine is the first phase to crystallise following magma ascent to lower pressure, thus recording the most primitive melt compositions and thereby inheriting Ni and Mn contents from the melt as a function of the contribution of peridotite and hybrid pyroxenite source lithologies. Olivines from Ocean Islands worldwide show a negative correlation between Ni and Mn and form a global array between low Ni, high Mn peridotite melts and high Ni, low Mn hybrid pyroxenite melts (Sobolev et al. 2005, 2007). This relationship between Ni and Mn, and therefore between peridotite and hybrid pyroxenite, can be exploited to determine the relative proportions of peridotite versus hybrid pyroxenite melts associated with a specific mantle source.

The geology and geochemistry of the Cape Verde archipelago

The Cape Verde archipelago is located approximately 500 km west of Senegal, Africa and consists of a 2 km high oceanic plateau, from which nine islands and a host of seamounts have developed (Fig. 1). The Cape Verde oceanic plateau is underlain by Cretaceous ocean crust (Ogg 1995; Ali and Watts 2003) and the islands form a westward opening horse-shoe shape arrangement.

The Cape Verde plateau is fed by a mantle upwelling that produces a thermal and topographic anomaly, a geoid anomaly and a seismic tomography anomaly that extends into the deep mantle, consistent with what is expected of a deep mantle plume (Courtney and White 1986; Ali and Watts 2003; Montelli et al. 2004, 2006; Pim et al. 2008).

The lavas from Cape Verde are highly alkaline, with the majority having compositions of basanites to melanephelinites (Davies et al. 1989; Le Bas 1989; Holm et al. 2006; Barker et al. 2009). The lavas range from aphyric, through olivine–clinopyroxene porphyritic to ankaramitic (Barker et al. 2009). Major and trace element compositions of the lavas suggest the involvement of pyroxenite to eclogite source lithologies in their genesis (Barker et al. 2009, 2010).

Not only do the islands form geographical groupings (i.e. northern, southern and eastern islands), but a geographical isotope heterogeneity is also apparent (Gerlach et al. 1988; Doucelance et al. 2003). The northern islands show high $^{206}Pb/^{204}Pb$ with negative $\Delta 8/4$, whereas the southern islands show lower $^{206}Pb/^{204}Pb$ and positive $\Delta 8/4$ (Gerlach et al. 1988). For that reason, the northern islands have been proposed to result from mixing between a HIMU-like source and a local DMM-like component (Gerlach et al. 1988; Holm et al. 2006). In contrast, the southern islands are considered to reflect the presence of an EM1-like component (Gerlach et al. 1988; Doucelance et al. 2003; Barker et al. 2009, 2010; Martins et al. 2009). The presence of the EM1-like component seems to be restricted to three of the southern islands (Maio, Santiago and Fogo), being absent at Brava until 0.5 Ma and from the Cadamosto Seamount furthest southwest (Barker et al. 2012; Mourão et al. 2012). Detailed studies of Santo Antão from the northern island group and Santiago from the southern island group have shown that the isotopic heterogeneity has persisted over at least 7.5 and 4.5 Myrs, respectively (Holm et al. 2006, 2008; Barker et al. 2009, 2010). The temporal geochemical record of samples for Santo Antão and Santiago shows uniform compositions for the local DMM-like and EM1-like components, whereas the HIMU-like component shows

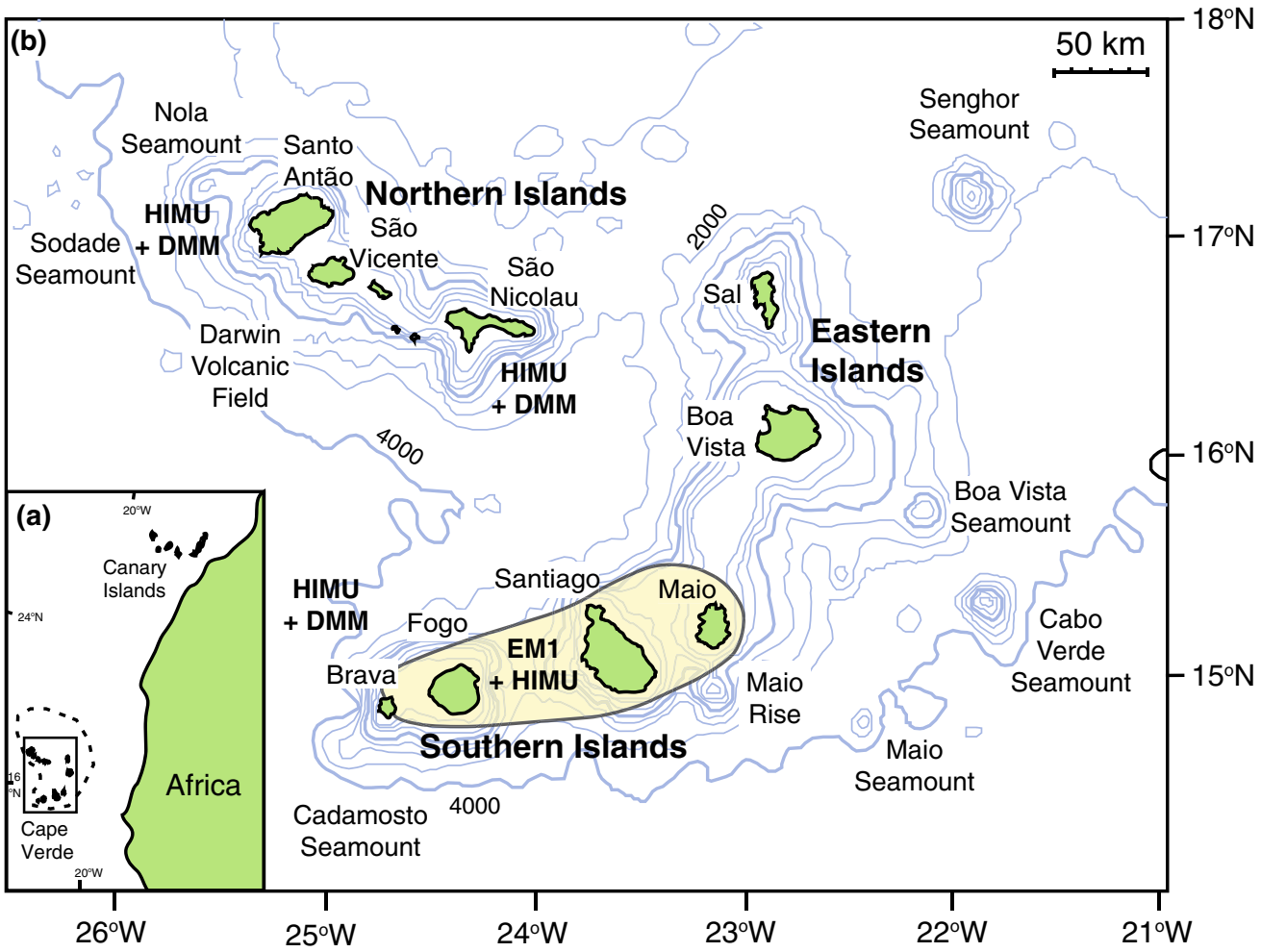

Fig. 1 **a** Location map of the Cape Verde oceanic plateau, approximately 500 km west of Africa. **b** Map of the Cape Verde archipelago showing the northern, southern and eastern island groups. The islands of Santo Antão, from the northern islands, and Santiago, from the southern islands, are the focus of this study. HIMU-like and local DMM-like mantle sources are dominant in the northern islands, eastern islands and the island of Brava and the Cadamosto Seamount, in the southwest of the archipelago (Gerlach et al. 1988; Doucelance et al. 2003; Holm et al. 2006; Millet et al. 2008; Hildner et al. 2011; Barker et al. 2012). The EM1-like component is restricted to the three of the southern islands; Maio, Santiago and Fogo plus in volcanics <0.5 Ma from Brava (Gerlach et al. 1988; Doucelance et al. 2003; Martins et al. 2009; Barker et al. 2009, 2010, 2012; Mourão et al. 2012)

a temporal change in $^{208}Pb/^{204}Pb$ across the Cape Verde archipelago (Barker et al. 2010).

A range of theories for the origin of the EM1-like component have been proposed including a subcontinental lithospheric mantle source derived from the African continental margin that was trapped in the oceanic lithosphere during formation of the ocean crust or resides in the upper mantle (Kokfelt et al. 1998; Abratis et al. 2002; Doucelance et al. 2003; Escrig et al. 2005; Geldmacher et al. 2008; Martins et al. 2009). Alternatively, the origin of the EM1-like component may be recycled inhomogeneous ocean crust sampled at depth by the mantle plume (Barker et al. 2010, 2012). If the oceanic lithospheric mantle hosts the EM1-like end-member, we would expect the magmas to be influenced by the EM1-like component as they travel through the lithosphere. However, extensive crystallisation has been shown to occur in the oceanic lithospheric mantle (Barker et al. 2009, 2012; Hildner et al. 2011), independent of the presence or absence of the EM1-like end-member. Furthermore, geochemical evidence for mixing of the EM1-like and HIMU-like sources during melting suggests the presence of both components in the melting column deep beneath the oceanic lithosphere (Barker et al. 2009).

Sample selection

The samples were selected based on their olivine content and represent the range of whole rock isotopic variations

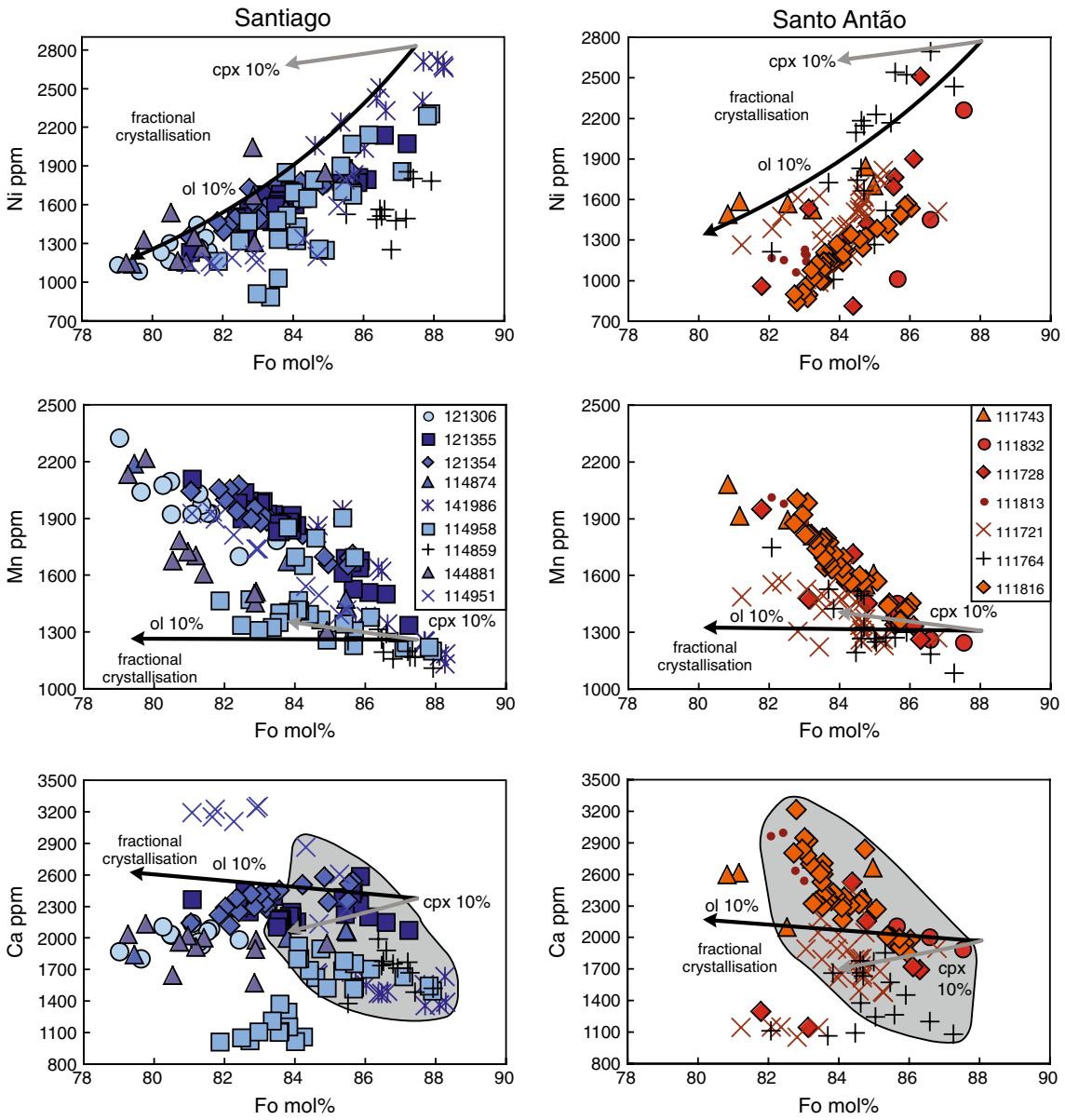

Fig. 2 Minor elements in olivine for the presented Cape Verde samples. The Ni, Mn and Ca concentrations in olivine versus forsterite (Fo) are shown for samples from Santiago and Santo Antão. Fractionation vectors are calculated for olivine and clinopyroxene using partition coefficients from Bougault and Hekinian (1974), Herzberg and O'Hara (2002), Adam and Green (2006). *Grey* fields outline the data filtered to eliminate the effects of clinopyroxene crystallisation

observed in lavas from Santo Antão and Santiago. The islands of Santo Antão and Santiago were chosen to represent the northern and southern islands of Cape Verde, respectively, due to their well characterised and temporally constrained sample suites (Holm et al. 2006; Barker et al. 2009, 2010). Furthermore, samples with the highest Mg#'s [$Mg/(Mg+Fe^{2+}+Fe^{3+})$ mol%] and olivine with magmatic Ca contents were selected. Samples known to have significant influence of crystal accumulation were avoided. However, several of the samples were not previously analysed for mineral chemistry, and therefore, analyses were checked for anomalously low Ca contents, similar to olivine from Cape Verde mantle xenoliths (0.04–0.29 wt%, mean 0.17 ± 0.1 wt% 2 SD Ryabchikov et al. 1995; Bonadiman et al. 2005). Several individual olivine cores in various samples showed low CaO contents (0.03–0.07 wt%), with others identified as falling below the CaO–Fo trend for a given Fo content ($n = 9/210$). These were considered to be xenocrystic olivine and therefore filtered from the dataset. Additionally, five more analyses were excluded based on very high or very low Fo contents with scattered CaO contents. The filtered dataset has olivine with a range of

CaO contents between 0.14 and 0.45 wt%, and a mean of 0.28 ± 0.14 wt% (2 SD; Fig. 2), which compares favourably to previously reported data for magmatic olivine from Cape Verde, that range from ca. 0.18 to 0.51 wt% (Barker et al. 2009).

Analytical method

Olivine phenocrysts were analysed using a JEOL Superprobe JXA-8200 electron microprobe at the University of Copenhagen. Analyses were performed with an accelerating voltage of 15 keV and beam current of 200 nA. The analytical protocol was similar to that of Sobolev et al. (2007), with the following modifications: High precision Ni and Mn data were acquired by peak counting times of 60 s, which were run in triplicate to provide an accumulated analysis time of 180 s which we calculate to a weighted mean. Detection limits are lower than 75 ppm for Ni, Mn and Ca and 2 sigma uncertainties are better than 5 %. Several samples were duplicated by analysis on the JEOL JXA-8530F Hyperprobe FEG-EPMA at CEMPEG, Uppsala University to confirm accuracy of analyses. The analytical uncertainties for the minor elements Ni, Mn, Ca were ≤4 % (1 SD), which equates to ca. 40 ppm.

The cores of the olivine phenocrysts were analysed to record crystallisation from the earliest possible melts. The analyses of olivine in each sample were averaged and are presented with the mean data per sample in Table 1, and the full dataset is given in the supplementary materials. The difference between the mean Mn/FeO and Ni*FeO/MgO for samples analysed at the University of Copenhagen and duplicated at Uppsala University is ≤12 %, whereas the distribution of the data around the mean Mn/FeO and Ni*FeO/MgO for individual samples are Mn/FeO of ±4 to ±28, (2 SD) and Ni*FeO/MgO of ±16 to ±256 (2 SD). Therefore, the duplicates are within error of the sample means, confirming the quality of the analytical data but also highlighting the inherent uncertainties in using mean olivine data for single samples.

The whole rock major element, trace element and radiogenic isotope data for the samples presented herein are described in Holm et al. (2006) and Barker et al. (2009, 2010).

Results

Olivine porphyritic samples used in this study range in whole rock MgO content from 8.3 to 13.6 wt% with one sample at 6.1 wt% for samples from Santiago and 7.3 to 18.5 wt% for samples from Santo Antão. The corresponding cores of olivine phenocrysts have Fo content of 79–88 and 81–89 % for samples from Santiago and Santo Antão, respectively (Fig. 2), with individual samples displaying ranges of 2.5–6.2 mol% Fo. Olivines from Santiago have Ni contents of 890–2,720 ppm, Mn contents of 1,110–2,330 ppm and Ca contents of 1,015–2,590 ppm (Fig. 2). Olivine phenocryst cores from Santo Antão have Ni contents of 810–2,700 ppm, Mn contents of 1,080–2,080 ppm and Ca contents of 1,050–3,220 ppm. Nickel concentrations form a positive trend, whereas Mn and Ca exhibit a negative trend with Fo contents. These relationships reflect fractional crystallisation of olivine which causes decreasing Ni and increasing Ca with decreasing Fo content, and the minor change in Mn contributes to the spread of the data away from the negative Mn–Fo trend. Additionally, clinopyroxene crystallisation leads to slightly increasing Mn and decreasing Ca content with decreasing Fo and minimal change in Ni, which causes scattering of the Ni–Fo trend (Fig. 2).

The dataset was tested for the effects of clinopyroxene crystallisation by filtering the samples that fall away from the trend of increasing Ca with decreasing Fo content, i.e. those outside the grey fields shown in Fig. 2.

Ratios of Ni*FeO/MgO, Mn/FeO and Ca/FeO show no correlation with Fo content, displaying a scattered appearance (Fig. 3). The variations in Ni*FeO/MgO and Mn/FeO are very similar between the entire dataset and those in the grey fields that eliminate clinopyroxene crystallisation. This similarity likely represents compositional diversity in the melts inherited from the source. Fractional crystallisation vectors show that olivine crystallisation can still decrease the Ni*FeO/MgO ratios and increase the Ca/FeO ratios, while clinopyroxene crystallisation will result in lower Ca/FeO ratios (Fig. 3).

The mean Ni*FeO/MgO and Mn/FeO ratios were calculated for individual samples and are plotted for the clinopyroxene crystallisation filtered data (Fig. 4a) and for the entire dataset (Fig. 4b). The range of the two datasets is very similar, showing Ni*FeO/MgO ratios of 382–637 and 384–636 and Mn/FeO ratios of 89–122 and 86–122 for unfiltered and filtered data, respectively. Furthermore, the filtered and unfiltered data are highly correlated, 0.993 for Mn/FeO (r^2 = 0.91) and 1.011 for Ni*FeO/MgO (r^2 = 0.91). The uncertainties of the mean Mn/FeO and Ni*FeO/MgO ratios are comparable, ranging between 4 and 26 (2 SD) for Mn/FeO for both datasets and 16–256 versus 14–266 (2 SD) for Ni*FeO/MgO for the full dataset and filtered dataset, respectively. Therefore, we favour the better statistical basis of the larger dataset upon which the following discussion will focus. Additionally, the simultaneous influence of fractional crystallisation on Ni*FeO/MgO and Mn/FeO is for olivine crystallisation to decrease the Ni*FeO/MgO ratio and slightly increase the Mn/FeO ratio (Fig. 4); meanwhile, clinopyroxene crystallisation would increase the Mn/FeO and Ni*FeO/MgO ratios

Table 1 Mean Fo content and concentrations of minor elements (Ni, Mn, Ca) and mean Mn/FeO and Ni*FeO/MgO in volcanics from Santiago and Santo Antão, Cape Verde

	Age group	Fo	2 SD	Ni (ppm)	2 SD	Mn (ppm)	2 SD	Ca (ppm)	2 SD	Mn/FeO	2 SD	Ni*FeO/MgO	2 SD	X_{ecl} (%)	$^{206}Pb/^{204}Pb$
Santiago															
121306	OV	81.1	2.4	1,322	348	1,970	312	1,987	294	110	9	546	72	22	19.140
121355	OV	84.1	3.6	1,643	482	1,797	446	2,341	234	117	9	544	58	3	19.464
121355UU	OV	83.7	0.4	1,645	70	1,866	46	2,174	82	122	4	570	24	0	19.464
121354	OV	83.4	2.8	1,608	312	1,878	280	2,360	258	118	5	567	54	0	19.485
114874	IV	83.5	5.6	1,555	582	1,691	698	1,992	210	107	10	533	16	30	19.127
114951	IV	83.2	3.2	1,289	450	1,689	422	2,903	842	106	9	457	82	42	19.257
114958	IV	84.3	2.0	1,726	288	1,288	64	1,326	590	86	7	570	82	77	19.430
114958UU	IV	84.7	3.0	1,605	852	1,333	158	1,470	570	93	13	507	194	65	19.430
141986	YV	86.6	2.4	2,329	686	1,424	556	1,496	330	110	28	636	126	8	19.425
114859	YV	86.8	5.8	1,574	636	1,215	626	1,698	862	96	12	425	78	65	19.189
114881	YV	81.6	3.4	1,439	602	1,693	552	1,918	332	97	18	572	168	50	18.819
Santo Antão															
111743	OV	82.9	3.4	1,620	262	1,810	398	2,515	478	112	8	593	92	10	19.884
111832	IV	87.1	2.2	1,727	948	1,339	186	2,300	690	108	14	449	202	39	19.173
111728	IV	84.6	3.0	1,546	1,020	1,497	436	1,872	918	102	15	489	248	47	19.746
111813	IV	83.1	1.8	1,187	122	1,920	172	2,912	402	120	7	429	42	15	19.892
111816	IV	85.5	1.6	1,449	246	1,446	178	2,012	312	104	6	438	32	48	19.360
111816UU	IV	83.7	1.2	1,110	280	1,736	232	2,514	498	112	9	384	70	37	19.360
111721	YV	84.1	2.0	1,446	452	1,412	318	1,723	696	93	20	486	144	66	19.610
111764	YV	84.9	2.4	1,940	996	1,353	330	1,444	562	94	14	606	250	57	19.773

The mean compositions have standard deviations of 8.3 ± 8.0 and 10.4 ± 7.0 % (1 SD) for the minor element concentrations and Mn/FeO and Ni*FeO/MgO

Radiogenic isotopes for the corresponding samples are from Holm et al. (2006), Barker et al. (2009, 2010)

X_{ecl} is the proportion of eclogite melt that contributes to the mean olivine composition for the samples

OV, IV, YV old, intermediate and young volcanics, respectively

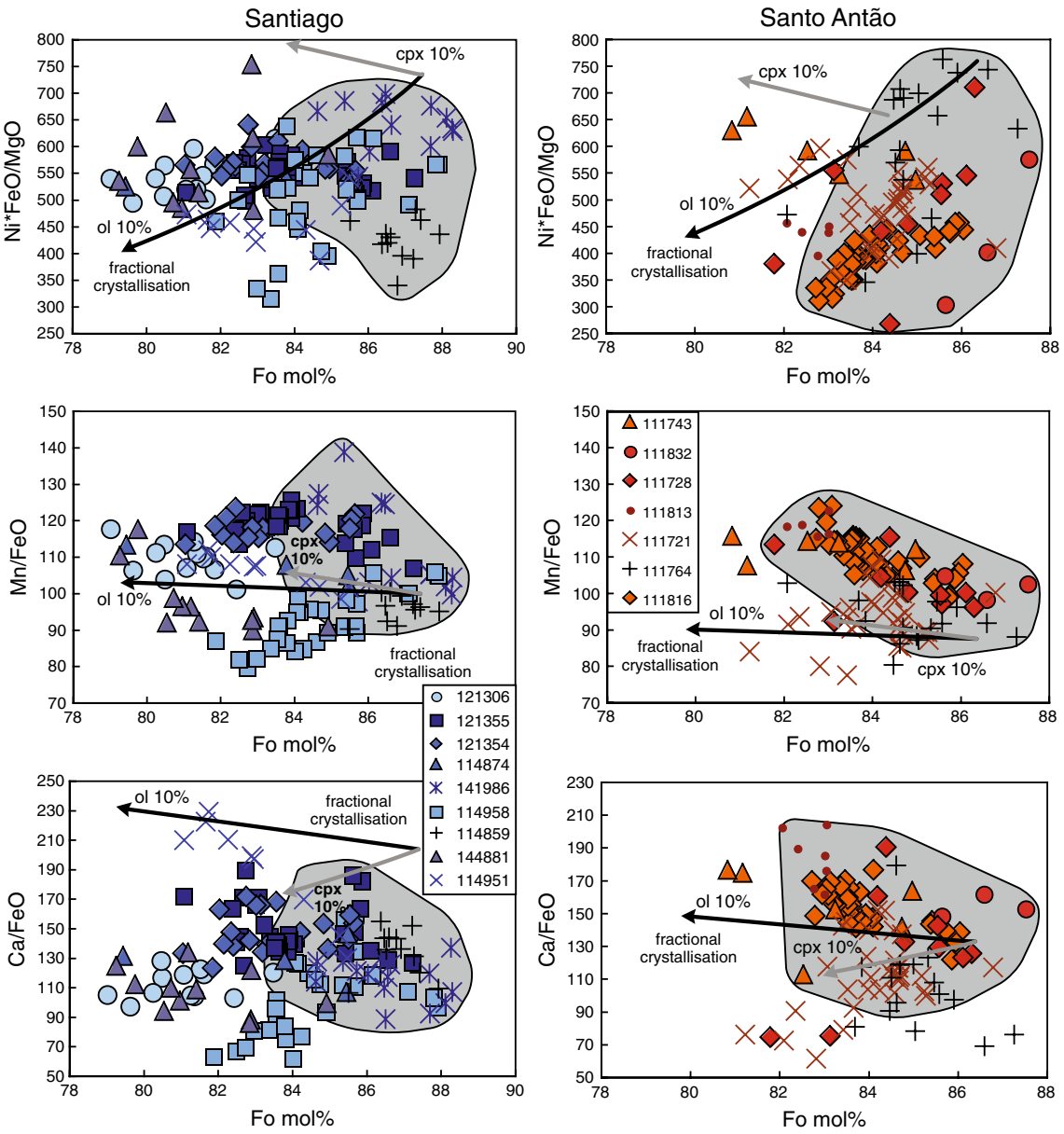

Fig. 3 Ratios of minor elements in olivine for the Cape Verde samples. The Ni*FeO/MgO, Mn/FeO and Ca/FeO ratios in olivine are shown versus forsterite (Fo) for samples from Santiago and Santo Antão. Fractionation vectors are calculated for olivine and clinopyroxene using partition coefficients from Bougault and Hekinian (1974), Herzberg and O'Hara (2002), Adam and Green (2006). *Grey* fields show the filtered data to eliminate the effects of clinopyroxene crystallisation

simultaneously. Therefore, the spread of the data from high to low Mn/FeO at low to intermediate Ni*FeO/MgO away from the global array contrasts with the sense of fractional crystallisation and cannot be considered a product of fractional crystallisation.

The olivine phenocrysts from the Santiago and Santo Antão volcanics range in mean Mn/FeO from high to low, where the corresponding mean Ni*FeO/MgO ratios are intermediate to low compared to the global array. Olivine from the old volcanics (OV) from Santiago and Santo Antão has Ni*FeO/MgO ratios of 545–590 and Mn/FeO ratios of 110–122, whereas olivine phenocrysts from the intermediate volcanics (IV) and young volcanics (YV) extend to much lower Mn/FeO ratios (Fig. 4). The intermediate volcanics from Santo Antão extend from intermediate Mn/Fe to high Mn/FeO at the lowest Ni*FeO/MgO ratios.

Whole rock TiO_2 concentrations range from 2.7 to 4.6 wt% for samples from Santiago and from 3.4 to 5.5 wt% for samples from Santo Antão. The whole rock TiO_2 generally increases with decreasing mean Mn/FeO

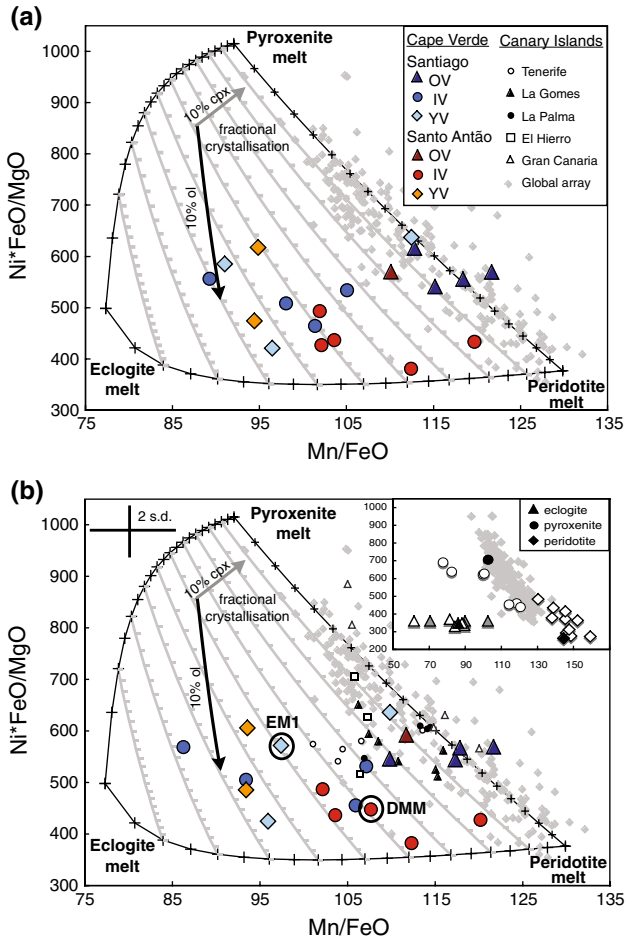

Fig. 4 **a** Mean Ni*FeO/MgO versus Mn/FeO for olivine phenocrysts filtered by Ca–Fo content for clinopyroxene crystallisation from lavas from Santiago and Santo Antão, Cape Verde. **b** Mean Ni*FeO/MgO versus Mn/FeO for lavas from Santiago and Santo Antão. The global array (*grey diamonds*) and lavas from the Canary Islands are shown for comparison (Sobolev et al. 2005, 2007; Gurenko et al. 2009, 2010a). Abbreviations: *OV* old volcanics, *IV* intermediate volcanics, *YV* young volcanics. The olivines from Cape Verde show a trend that deviates from the global array towards low Mn/FeO and Ni*FeO/MgO. The experimental melts for peridotite, pyroxenite and eclogite are shown in *white or grey* in the *inset*, the selected end-members are in *black* (Sobolev et al. 2005, 2007; Pertermann and Hirschmann 2002; Dasgupta et al. 2006 (*grey*)). The Ni*FeO/MgO for the eclogites is calculated based on applying the single Ni analyses to each eclogite sample. Peridotite and pyroxenite end-member melts are the best-fit values for the global array from data presented in Sobolev et al. (2005, 2007) and eclogite from Pertermann and Hirschmann (2002). Partition coefficients are MgO = 3.23 (Beattie 1994), FeO = 0.9 (Kloeck and Palme 1988), MnO = 0.809 (Herzberg and O'Hara 2002) and NiO = 5.14 (Sobolev et al. 2005). The model is built up from binary mixing of the melts recalculated into olivine compositions. Ternary mixing grid is constructed to show 5 % intervals and the grey lines delineating X_{ecl} are shown for 10 % intervals

ratios in olivines, with a large range in Mn/FeO ratios towards high TiO_2 contents (Fig. 5). Whole rock TiO_2 contents form two distinct trends with Ni*FeO/MgO, one with high Ni*FeO/MgO of 505–640 at TiO_2 of 2.7–4.5 wt% and another at low Ni*FeO/MgO of 350–490 with TiO_2 of 3.3–5.5 wt%. Ratios of La/Nb range from 0.44 to 0.73 in samples from Santiago and form positive trends with mean Ni*FeO/MgO and Mn/FeO of corresponding olivine. The La/Nb ratios for samples from Santo Antão fall uniformly between 0.74 and 0.84 over the range of mean Ni*FeO/MgO and Mn/FeO for corresponding olivines. One sample, however, plots at La/Nb of 0.61, low Ni*FeO/MgO of 450, and displays an intermediate Mn/FeO ratio of 108.

The Pb isotopes for Santiago and Santo Antão range from $^{206}Pb/^{204}Pb$ 18.8 to 19.9, with Santiago having positive Δ8/4 at lower $^{206}Pb/^{204}Pb$ of 18.8–19.5 than Santo Antão, which shows higher $^{206}Pb/^{204}Pb$ of 19.2–19.9 at negative Δ8/4 (Gerlach et al. 1988; Doucelance et al. 2003; Holm et al. 2006; Barker et al. 2009, 2010). The low $^{206}Pb/^{204}Pb$ end-members of the Santiago ($^{206}Pb/^{204}Pb$ = 18.8) and Santo Antão ($^{206}Pb/^{204}Pb$ = 19.2) have olivine with mean Ni*FeO/MgO of 572 and 450, and mean Mn/FeO of 97 and 108, respectively (Fig. 6). The high $^{206}Pb/^{204}Pb$ end-members of the Santiago ($^{206}Pb/^{204}Pb$ = 19.5) and Santo Antão ($^{206}Pb/^{204}Pb$ = 19.7–19.9) samples have a wide range in olivine compositions, with mean Ni*FeO/MgO of 507–636 and 429–606 and mean Mn/FeO of 96–122 and 94–120, respectively. The intermediate $^{206}Pb/^{204}Pb$ lavas generally have intermediate Mn/FeO and Ni*FeO/MgO with two samples from Santiago plotting at low Ni*FeO/MgO ratios of 425–460 (Fig. 6; $^{206}Pb/^{204}Pb$ of 19.1–19.3).

Discussion

Relationships amongst peridotite, pyroxenite and eclogite melts at Cape Verde

The global array of Mn/FeO versus Ni*FeO/MgO for olivine shows a strong negative correlation. This relationship represents mixing between melts from a peridotite source with high Mn/FeO and low Ni*FeO/MgO and an olivine-free hybrid pyroxenite source produced by reaction between an eclogite melt and peridotite, which is characterised by high Ni*FeO/MgO and low Mn/FeO (Fig. 4; Sobolev et al. 2005, 2007). The olivine phenocrysts from Cape Verde plot partly along the global array at intermediate Mn/FeO and Ni*FeO/MgO, but the majority of the samples fall to low Mn/FeO and Ni*FeO/MgO, away from the peridotite–hybrid pyroxenite mixing line (Fig. 4). This trend to low Mn/FeO and Ni*FeO/MgO suggests involvement of another source lithology, one that produces low Mn/FeO melts and has not inherited high Ni*FeO/MgO. One option would be partial melts from an eclogite source that are expected to have correspondingly low Mn/FeO, as found in a range of eclogites including carbonated eclogite, which also provides a suitable whole rock composition for

the Cape Verde lavas (61–103 with a mean of 83 Mn/FeO; Pertermann and Hirschmann 2002; Dasgupta et al. 2006; Barker et al. 2009). This observation is consistent with the theoretical basis to expect low Mn/FeO from an eclogite melt due to retention of Mn by garnet during melting and also low Ni*FeO/MgO due to the lack of a Ni-bearing phase. The limited evidence of Ni concentration of eclogite melts also suggests that they would have low Ni*FeO/MgO (360; Pertermann and Hirschmann 2002) and would thus provide a suitable source. The influence of eclogite is also apparent in the variations of minor elements in olivine with the whole rock compositions, where low Mn/FeO and Ni*FeO/MgO are associated with relatively high TiO_2 and low La/Nb. The La/Nb ratio highlights the partitioning due to source composition as opposed to melting processes with low values being distinctive of pyroxenite/eclogite sources and therefore, combined with high TiO_2 compositions, likely reflects less influence of peridotite (Fig. 5; Prytulak and Elliott 2007; Stracke and Bourdon 2009).

The observed deviation from the global array to low Mn/FeO melts at low Ni*FeO/MgO towards an eclogitic source is likely a reflection of the dynamics of the mantle plume and melting column below Cape Verde. If there was large-scale flow, then the mantle would be well mixed and the eclogite melt would react with the peridotite, typical for Ocean Island Basalt. However, if the eclogite heterogeneities were large enough (>0.1–1 m), the melts could potentially escape without undergoing melt-peridotite reaction (Kogiso et al. 2004b; Sobolev et al. 2005). Furthermore, if the melt-peridotite reaction forms a reaction aureole, the melt pathways may be sealed off from the surrounding peridotite precluding further melt-peridotite reaction (Kogiso et al. 2004b), and a combination of these processes may cause the efficient extraction of eclogite melts beneath Cape Verde.

An alternative option could be the interaction of a silica undersaturated melt with the oceanic lithospheric mantle, whereby the melt would dissolve orthopyroxene and crystallise olivine (cf. Kelemen et al. 1998). This would be expected to lead to melt and olivine phenocrysts with low Ni*FeO/MgO reflecting the low Ni content of orthopyroxene. However, above the garnet stability field the melt and corresponding olivine would likely not be restricted to low Mn/FeO ratios. Indeed, lherzolite and harzburgite xenoliths from Cape Verde and the Canary Islands have olivine

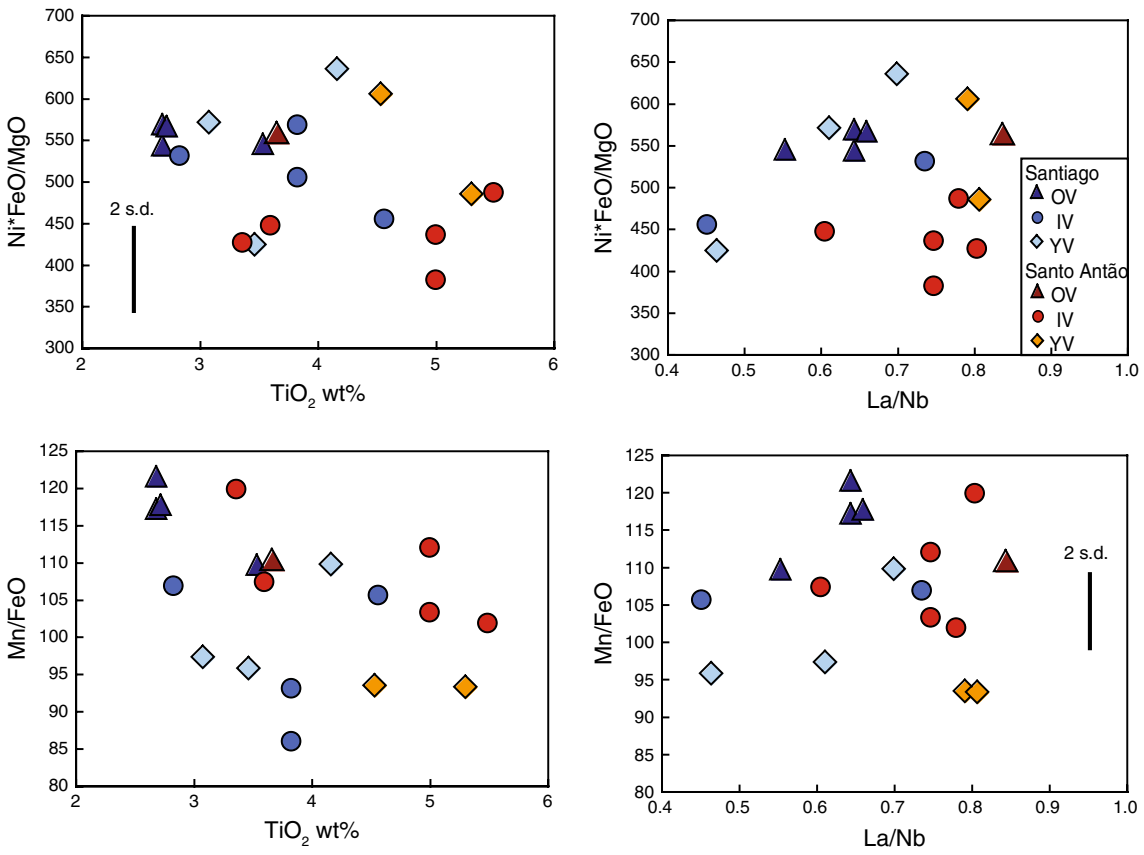

Fig. 5 Minor elements in olivine versus TiO_2 and La/Nb of the respective whole rocks for the Santiago and Santo Antão lavas. Mean Ni*FeO/MgO and Mn/FeO ratios of each sample are shown and have average uncertainties of 10 and 100, respectively (2 SD). Abbreviations: *OV* old volcanics, *IV* intermediate volcanics, *YV* young volcanics

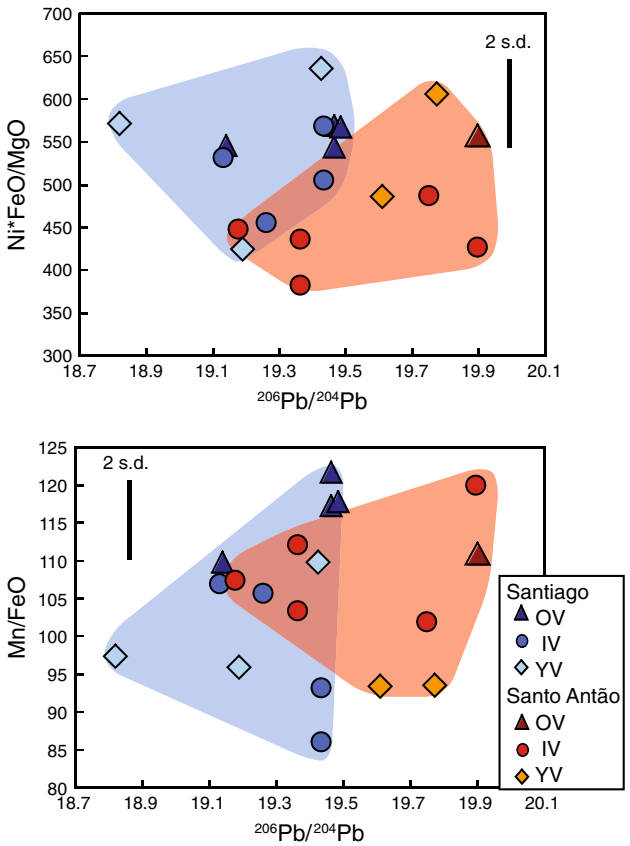

Fig. 6 Variations in minor elements in olivine (mean Mn/FeO and Ni*FeO/MgO) with whole rock $^{206}Pb/^{204}Pb$. A wide variation in Mn/FeO and Ni*FeO/MgO is observed in olivine from host lavas with high $^{206}Pb/^{204}Pb$ for both Santiago and Santo Antão. Abbreviations: *OV* old volcanics, *IV* intermediate volcanics, *YV* young volcanics

compositions with a wide range of Mn/FeO ratios from 86 to 172 and similar orthopyroxene compositions (Neumann et al. 2000; Bonadiman et al. 2005). Such xenolith compositions extend well beyond the olivine compositions with low Mn/FeO of 86–122 observed in the Cape Verde lavas. Intriguingly, the Ni*FeO/MgO ratios are lower for the Cape Verde lherzolite and harzburgite xenoliths (278–457) than for the Canary Islands harzburgite xenoliths (514–674; Neumann et al. 2000; Bonadiman et al. 2005). Therefore, the oceanic lithospheric mantle provides one plausible option for generating low Ni*FeO/MgO melts, but the restriction of our data to low Mn/FeO contents in comparison with the wide range shown by the mantle xenoliths from Cape Verde and the Canary Islands causes us to favour an origin from eclogite melt in the asthenospheric mantle.

Quantification of melt contributions

The involvement of a third, eclogitic melt requires a more complex approach to quantification of melt contributions. We have modelled mixing between peridotite, pyroxenite and eclogite melts as a binary-mixing system between melts of each of the three components. The end-members representing the peridotite and pyroxenite melts are from Sobolev et al. (2005, 2007), where the compositions that lead to the best fit for the global array were chosen (inset Fig. 4b). Limited experimental studies have measured Ni on eclogite melts; therefore, the eclogite melt from Pertermann and Hirschmann (2002) was chosen. This eclogite melt has similar Mn/FeO composition to the carbonated eclogite melts of Dasgupta et al. (2006), which provide a reasonably good match for the major element compositions of the Cape Verde lavas (Barker et al. 2009). Partition coefficients were then used to calculate the corresponding olivine compositions for plotting as a ternary mixing grid. Following Sobolev et al. (2005), the same partition coefficients were used for olivine-melt from peridotite and pyroxenite, this was then extended to olivine crystallising from eclogite melts due to lack of alternative partition coefficients (olivine-melt partition coefficients from: Sobolev et al. 2005; Herzberg and O'Hara 2002; Beattie 1994; Kloeck and Palme 1988). The actual melts will likely have mixed by the time of olivine crystallisation; hence, they will not be pure eclogite, pyroxenite or peridotite melts, and therefore, it is considered reasonable to assume that the olivine-melt partition coefficients for peridotite are representative. Moreover, fixed partition coefficients were used in order to be consistent with the use of the most recent olivine-melt partition coefficient for Ni from Sobolev et al. (2005). The majority of the samples from Cape Verde trend away from the peridotite–pyroxenite global array and towards melts from an eclogite source. The Cape Verde olivine data are modelled to have formed from melts of 5–75 % peridotite, 0–50 % pyroxenite and 0–77 % eclogite (Fig. 4). The composition of olivine from Santiago and Santo Antão shows similar ranges in source melts, with olivine phenocrysts of the intermediate volcanics at Santo Antão extending from average peridotite melt contributions of 45 % towards peridotite melts of $\leq$75 %, consistent with the involvement of a local DMM-like source (Fig. 4). The recognition that the Cape Verde lavas have experienced significant contributions of eclogite melt is consistent with comparison to experimental melts that indicate a potential role for carbonated eclogite in the generation of the Cape Verde lavas (Dasgupta et al. 2006; Barker et al. 2009).

We therefore interpret the trend of the Cape Verde olivine phenocrysts towards low Mn/FeO and Ni*FeO/MgO and away from the global array to indicate involvement of an eclogite melt which has escaped reaction with peridotite to form hybrid pyroxenite (Kogiso et al. 2004b; Stracke and Bourdon 2009; Herzberg 2011). Once the source lithologies have melted, the peridotite and eclogite-derived melts are apparently able to mix congruently, in contrast to eclogite

melt that encounters solid peridotite which will react to form hybrid pyroxenite. Congruent mixing of eclogite and peridotite melts can either be envisioned to occur shallower in the melting column or in the presence of carbonated peridotite which would also melt deeper in the mantle (Dasgupta et al. 2007; Stracke and Bourdon 2009; Herzberg 2011). Thus, hybrid pyroxenite and eclogite melts have distinct geochemical signatures. Indications of involvement of ≤77 % from eclogite melt suggest that the eclogite melts become progressively more efficient at escaping from melt-peridotite reactions, and hence, less hybrid pyroxenite can form (cf. Kogiso et al. 2004b; Stracke and Bourdon 2009; Herzberg 2011). Moreover, the melting region is likely not well mixed, probably allowing eclogite to react with peridotite in small pockets only, i.e. along the contacts of the melt with the surrounding peridotite, which perhaps become sealed to further melt-peridotite reaction by formation of a reaction aureole (Kogiso et al. 2004b; Stracke and Bourdon 2009; Herzberg 2011). Therefore, the formation of hybrid pyroxenite could be a localised phenomena, where eclogite melts are able to escape melt-peridotite reaction as a function of the heterogeneity size and seal off the melt pathways from the surrounding peridotite.

The connection between the origin of melts and mantle source components

The Cape Verde volcanics from Santiago and Santo Antão are derived from three mantle sources (Gerlach et al. 1988). These can be represented by Pb isotopes, with the high $^{206}Pb/^{204}Pb$ representing a HIMU-like source, the low $^{206}Pb/^{204}Pb$ end-member in Santiago (18.8) reflecting an EM1-like source and the low $^{206}Pb/^{204}Pb$ from Santo Antão originating from a local DMM-like source (Gerlach et al. 1988; Doucelance et al. 2003; Holm et al. 2006; Martins et al. 2009; Barker et al. 2009, 2010).

The challenge of connecting melt contributions to source lithologies is complicated by the processes of melting, melt-peridotite reaction, sealing of the pathways from reaction with the peridotite, melt extraction without melt-peridotite reaction and size of the heterogeneities. Hence, we can only draw interpretations of the proportions of peridotite, pyroxenite and eclogite melt that contributed to the resulting lavas but not the proportions of the lithologies in the mantle source.

The involvement of melts from three sources with variable Mn/FeO and Ni*FeO/MgO makes it difficult to represent the variations with Pb isotopes. Thus, we assign each sample an X_{ecl} melt value based on the relationship between Mn/FeO and Ni*FeO/MgO, in accordance with the ternary mixing relationship between peridotite, hybrid pyroxenite and eclogite melts (Figs. 4, 7; Table 1).

The EM1-like end-member with the lowest $^{206}Pb/^{204}Pb$ is associated with a mixed peridotite–pyroxenite–eclogite

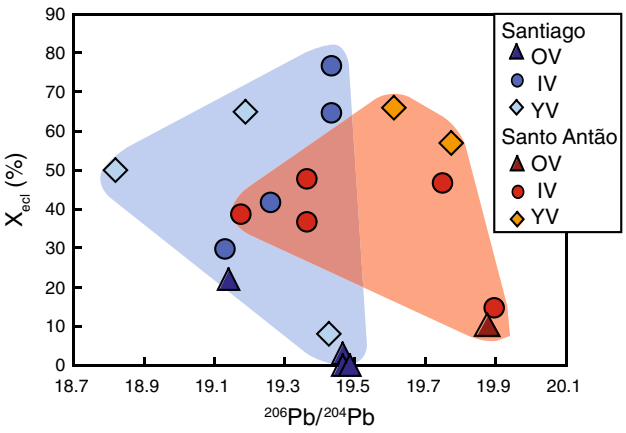

Fig. 7 The proportion of eclogite melt (X_{ecl}) that contributed to mean olivine composition is plotted versus whole rock $^{206}Pb/^{204}Pb$ for the Cape Verde lavas. The low $^{206}Pb/^{204}Pb$ EM1-like end-member of the Santiago samples has X_{ecl} of ca. 50 %, and the low $^{206}Pb/^{204}Pb$ local DMM-like end-member of the Santo Antão samples has X_{ecl} of ca. 40 %. The high $^{206}Pb/^{204}Pb$ HIMU-like samples from Santiago and Santo Antão show a wide range in X_{ecl} with values from 0 to 77 %. Abbreviations: *OV* old volcanics, *IV* intermediate volcanics, *YV* young volcanics

melt, with the mean olivine compositions showing contributions from ca. 25 % peridotite, ca. 25 % pyroxenite and ca. 50 % eclogite melts (Figs. 4b, 7). The local DMM-like end-member, the lowest $^{206}Pb/^{204}Pb$ from Santo Antão (red circle), shows a larger proportion of peridotite melt than the EM1-like source, with contributions of 47 % peridotite, 14 % pyroxenite and 39 % eclogite melts (Figs. 4b, 7). The HIMU-like component sampled in both Santo Antão and Santiago shows a wide range of contributions from eclogite melts from virtually none to a large proportion, associated with 5–75 % peridotite, 0–45 % pyroxenite and 0–77 % eclogite (Figs. 4b, 7). We argue below that the contribution of eclogite melt to the HIMU-like component varies as a function of time, thus explaining this large variation in a systematic way.

All three of these mantle sources, including the EM1-like end-member, show involvement of eclogite melts in their source. Eclogite begins to melt deeper than peridotite (Yaxley and Green 1998) and is thus present in the melting column to react with the peridotite and generate hybrid pyroxenite. This observation challenges the notion of deriving the EM1-like end-member from small heterogeneities trapped in the oceanic lithosphere following break-up of the African continental margin (e.g. Abratis et al. 2002; Escrig et al. 2005).

Temporal variations in source melts

The volcanics from Santiago and Santo Antão exhibit a synchronous archipelago wide change in $^{208}Pb/^{204}Pb$ of the high $^{206}Pb/^{204}Pb$ HIMU-like component with time

(Barker et al. 2010), with the intermediate and young volcanics showing lower $^{208}Pb/^{204}Pb$ than the old volcanics. Such temporal variation is also apparent in the minor elements in olivine data presented here. We find that the old volcanics (triangles; Fig. 4) have relatively high mean of Mn/FeO and Ni*FeO/MgO, where as the intermediate and young volcanics extend towards low mean of Mn/FeO and Ni*FeO/MgO (circles and diamonds, respectively, Fig. 4). This equates to a variation in the involvement of the eclogite melts, determined from mean olivine compositions, from ≤22 % in the old volcanics to ≤77 % in the intermediate and young volcanics (Fig. 7). This temporal change represents an increase in eclogite-derived melt with time, or an increased efficiency of eclogite melt extraction, perhaps promoted by a tendency for sealing of the eclogite melt pathways from reaction with peridotite. The intermediate volcanics on Santo Antão extend towards high Mn/FeO, and therefore, mean olivine compositions reflect 75 % peridotite, 10 % pyroxenite and 15 % eclogite melt contributions, suggesting a temporally and spatially restricted behaviour.

Comparison to the Canary Islands

The Canary Islands are very well characterised in terms of whole rock geochemistry, including radiogenic isotopes (e.g. Hoernle and Tilton 1991; Hoernle et al. 1991, 1995; Thirlwall 1997; Widom et al. 1999; Simonsen et al. 2000; Lundstrom et al. 2003; Gurenko et al. 2006; Deegan et al. 2012). In addition, there have been three recent studies focusing on the minor element compositions of olivines and the relationship between the source lithologies and mantle sources (Gurenko et al. 2009, 2010a, b). The respective data are plotted in Fig. 4b for comparison with the Cape Verde olivine phenocrysts. The Canary Island data generally follow the global trend plotting amongst the old volcanics from Cape Verde and extending to higher Ni*FeO/MgO and lower Mn/FeO and are therefore more enriched in hybrid pyroxenite than the Cape Verde samples. The samples from Tenerife plot to relatively lower Ni*FeO/MgO and Mn/FeO (Gurenko et al. 2009), similar to some of the intermediate and young volcanics from Cape Verde. This observation for Tenerife may hint at a small influence of eclogite melt that is efficiently extracted before peridotite-melt reaction occurs, limited interaction with the peridotite due to less efficient mantle flow or protection from peridotite-melt reaction by sealing of melt pathways. The samples from Gran Canaria plot to the lowest Mn/FeO and highest Ni*FeO/MgO for the Canary Islands (Gurenko et al. 2010a), suggesting a greater involvement of hybrid pyroxenite derived magmas than at the other Canary Islands, perhaps reflecting locally intensified mantle flow and a well-mixed mantle source.

Gurenko et al. (2009, 2010a) draw the conclusion of four end-member compositions for the Canary Islands, on coupling of isotopic end-members with source melts. These

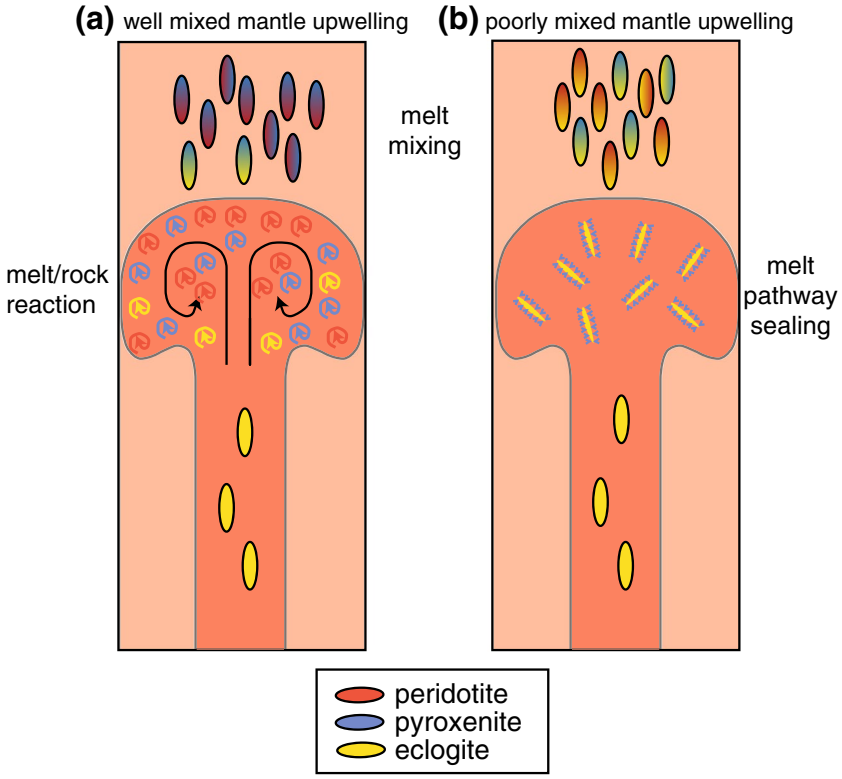

Fig. 8 Schematic illustration of the upwelling heterogeneities in the asthenosphere; **a** efficient mantle flow produces a well-mixed upwelling where eclogite melt reacts with peridotite to generate pyroxenite typical of Ocean Islands, e.g. the Canary Islands, **b** in areas of more sluggish mantle flow, larger heterogeneities are preserved, e.g. Cape Verde. Eclogite melts react with the peridotite and seal the eclogite heterogeneities from further melt-peridotite reaction, allowing efficient extraction of eclogite-derived melts. In the melting column, above the mantle upwelling, melts of different compositions are juxtaposed and mix congruently

are peridotite-rich HIMU-1, pyroxenite-rich HIMU-2, peridotite-rich EM1 and pyroxenite-rich DMM (Gurenko et al. 2009, 2010a). In contrast, the Cape Verde samples show melt derived from mixed peridotite–pyroxenite–eclogite for the EM1-like end-member, while the local DMM-like end-member is represented by a higher proportion of peridotite derived melt, and the HIMU-like end-member changes with time from an even mix of peridotite–pyroxenite melts to an increasing proportion of eclogite-derived melts.

A comparison between the source lithologies and mantle end-members of Ocean Island Basalts such as the Canary Islands versus Cape Verde is illustrated in Fig. 8. Typical Ocean Island Basalts have a peridotite upwelling hosting eclogite heterogeneities in an environment with efficient mantle flow, likely allowing the eclogite melts to react with peridotite to produce hybrid pyroxenite. This scenario contributes in various proportions to the magmas produced depending upon the supply of eclogite to form hybrid pyroxenite (Sobolev et al. 2005, 2007; Gurenko et al. 2009, 2010a). In contrast, at Cape Verde, the dynamics of the mantle upwelling are different, likely showing more sluggish mantle flow; therefore, the mixing of the heterogeneities will be less efficient preserving larger eclogite heterogeneities and allowing eclogite melts to escape from reaction with peridotite. Over time, the melt pathways are likely progressively sealed off in this relatively static environment, thus restricting melt-peridotite reaction further and hence promoting the extraction of eclogite-derived melts.

Conclusions

Cores of olivine phenocrysts hosted in primitive lavas from Cape Verde have minor element compositions that deviate from the global array towards low Mn/FeO and low Ni*FeO/MgO and are probably associated with an eclogite source. The occurrence of volcanics that record a contribution from eclogite melts is likely due to inhibited peridotite-melt reaction. Where peridotite-melt reaction is absent, the eclogite melt is extracted due to heterogeneity size and sluggish mantle flow or due to sealing of the melt pathways from the surrounding peridotite. The eclogite-derived melts then mix with peridotite and pyroxenite melts and contribute directly to the formation of Cape Verde magmas. The contribution of the source melts has been determined for the end-member isotopic heterogeneities of the Cape Verde volcanics, implying: (1) significant contribution of peridotitic melts associated with the local DMM-like source, (2) mixed peridotite–pyroxenite–eclogite melts representing the EM1-like component and (3) a wide range from an even mix of peridotite–pyroxenite derived melts towards eclogite dominated melts for the HIMU-like mantle component. A temporal change towards increasing eclogite-derived melt contributions throughout the Cape Verde archipelago appears to exist, implying that the eclogite melts are not just more efficiently extracted on a local scale but on an archipelago scale.

Acknowledgments Our thanks go to Alfons Berger for analytical advice and assistance. We are grateful for discussions with Kaj Hoernle, Thor Hansteen, Alexander Sobolev, Andrey Gurenko, Catherine Chauvel and Hans-Ulrich Schmincke, whose input greatly improved the manuscript. This research was supported by the Swedish National Research Council (Vetenskapprådet) in the form of Grant (Dnr: 2009-4316) to Barker and Troll.

References

Abouchami W, Hofmann AW, Galer SJG, Frey FA, Eisele J, Feigenson M (2005) Lead isotopes reveal bilateral asymmetry and vertical discontinuity in the Hawaiian mantle plume. Nature 434:851–856

Abratis M, Schmincke H-U, Hansteen TH (2002) Composition and evolution of submarine volcanic rocks from the central and western Canary Islands. Int J Earth Sci 91:562–582. doi:10.1007/s00531-002-0286-7

Adam J, Green T (2006) Trace element partitioning between mica- and amphibole-bearing garnet lherzolite and hydrous basanitic melt: 1. Experimental results and the investigation of controls on partitioning behavior. Contrib Miner Petrol 152:1–17

Ali MY, Watts AB (2003) A seismic reflection profile study of lithospheric flexure in the vicinity of the Cape Verde Islands. J Geophys Res 108:2239–2263

Barker AK, Holm PM, Peate DW, Baker JA (2009) Geochemical stratigraphy of submarine lavas (3–5 Ma) from the Flamengos Valley, Santiago, Cape Verde. J Petrol 50:169–193. doi:10.1093/petrology/egn081

Barker AK, Holm PM, Peate DW, Baker JA (2010) A 5 million year record of compositional variations in mantle sources to magmatism on Santiago, southern Cape Verde archipelago. Contrib Mineral Petrol 160:133–154. doi:10.1007/s00410-009-0470-x

Barker AK, Troll VR, Ellam RM, Hansteen TH, Harris C, Stillman CJ, Andersson A (2012) Magmatic evolution of the Cadamosto Seamount, Cape Verde: beyond the spatial extent of EM1. Contrib Mineral Petrol. doi:10.1007/s00410-011-0708-2

Beattie P (1994) Systematics and energetics of trace-element partitioning between olivine and silicate melts: implications for the nature of mineral/melt partitioning. Chem Geol 117:57–71. doi:10.1016/0009-2541(94)90121-X

Bonadiman C, Beccaluva L, Coltorti M, Siens F (2005) Kimberlite-like metasomatism and 'Garnet signature' in spinel-peridotite xenoliths from Sal, Cape Verde archipelago: relics of a subcontinental mantle domain within the Atlantic Ocean lithosphere? J Petrol 46:2465–2493

Bougault H, Hekinian R (1974) Rift valley in the Atlantic Ocean near 36 degrees 50′N; petrology and geochemistry of basalt rocks. Earth Planet Sci Lett 24(2):249–261. doi:10.1016/0012-821X(74)90103-4

Courtney RC, White RS (1986) Anomalous heat-flow and geoid across the Cape Verde Rise: evidence for dynamic support from a thermal plume in the mantle. Geophys J Royal Astr Soc 87:815–867

Dasgupta R, Hirschmann MM, Stalker K (2006) Immiscible transition from carbonate-rich to silicate-rich melts in the 3 GPa melting

interval of eclogite + CO_2 and genesis of silica-undersaturated ocean island lavas. J Petrol 47:647–671

Dasgupta R, Hirschmann MM, Smith ND (2007) Partial melting experiments of peridotite + CO_2 and genesis of alkalic ocean island basalts. J Petrol 48:2093–2124

Davies GR, Norry MJ, Gerlach DC, Cliff RA (1989) A combined chemical and Pb–Sr–Nd isotope study of the Azores and Cape Verde hot-spots: the geodynamic implications. In: Saunders AD, Norry MJ (eds) Magmatism in Ocean Basins, vol 42. Geological Society, London, Special Publications, pp 231–255

Deegan FM, Troll VR, Barker AK, Harris C, Chadwick JP, Carracedo JC, Delcamp A (2012) Crustal versus source processes recorded in dykes from the Northeast volcanic rift zone of Tenerife, Canary Islands. Chem Geol 334:324–344. doi:10.1016/j.chemgeo.2012.10.013

Doucelance R, Escrig S, Moriera M, Gariepy C, Kurz M (2003) Pb–Sr–He isotope and trace element geochemistry of the Cape Verde Archipelago. Geochim et Cosmochim Acta 67:3717–3733

Eisele J, Abouchami W, Galer SJG, Hofmann AW (2003) The 320 kyr Pb isotope evolution of Mauna Kea lavas recorded in the HSDP-2 drill core. Geochem Geophys Geosyst 4:8710. doi:10.1029/2002GC000339

Escrig S, Doucelance R, Moreira M, Allégre C (2005) Os isotope systematics in Fogo Island: evidence for lower continental crust fragments under the Cape Verde Southern Islands. Chem Geol 219:93–113

Geist DJ, White WM, McBirney AR (1988) Plume–asthenosphere mixing beneath the Galapagos archipelago. Nature 333:657–660

Geldmacher J, Hoernle K, Klügel A, van den Bogaard P, Bindeman I (2008) Geochemistry of a new enriched mantle type locality in the northern hemisphere: implications for the origin of the EM-1 source. Earth Planet Sci Lett 265:167–182

Gerlach DC, Cliff RA, Davies GR, Norry M, Hodgson N (1988) Magma sources of the Cape Verdes archipelago: isotopic and trace element constraints. Geochim et Cosmochim Acta 52:2979–2992

Gurenko AA, Hoernle KA, Hauff F, Schmincke H-U, Han D, Miura YN, Kaneoka I (2006) Major, trace element and Nd–Sr–Pb–O–He–Ar isotope signatures of shield stage lavas from the central and western Canary Islands: insights into mantle and crustal processes. Chem Geol 233:75–112

Gurenko AA, Sobolev AV, Hoernle KA, Hauff F, Schminke H-U (2009) Enriched, HIMU-type peridotite and depleted recycled pyroxenite in the Canary plume: a mixed-up mantle. Earth Planet Sci Lett 277:514–524. doi:10.1016/j.epsl.2008.11.013

Gurenko AA, Hoernle KA, Sobolev AV, Hauff F, Schminke H-U (2010a) Source components of the Gran Canaria (Canary Islands) shield stage magmas: evidence from olivine composition and Sr–Nd–Pb isotopes. Contrib Mineral Petrol 159:689–702. doi:10.1007/s00410-009-0448-8

Gurenko AA, Bindeman IN, Chaussidon M (2010b) Oxygen isotope heterogeneity of the mantle beneath the Canary Islands: insights from olivine phenocrysts. Contrib Mineral Petrol. doi:10.1007/s00410-010-0600-5

Hart SR (1984) A large-scale isotopic anomaly in the southern hemisphere mantle. Nature 309:753–757

Herzberg C (2011) Identification of source lithology in the Hawaiian and Canary Islands: implications for origins. J Petrol 52:113–146. doi:10.1093/petrology/egq075

Herzberg C, O'Hara MJ (2002) Plume-associated ultramafic magmas of Phanerozoic age. J Petrol 43:1857–1883

Hildner E, Klügel A, Hauff F (2011) Magma storage and ascent during the 1995 eruption of Fogo, Cape Verde archipelago. Contrib Mineral Petrol. doi:10.1007/s00410-011-0623-6

Hirose K, Kushiro I (1993) Partial melting of dry peridotites at high pressure; determination of composition of melts segregated from peridotite using aggregates of diamond. Earth Planet. Sci Lett 114:447–489

Hirschmann MM, Kogiso T, Baker MB, Stolper EM (2003) Alkalic magmas generated by partial melting of garnet pyroxenite. Geology 31:481–484

Hoernle K, Tilton GR (1991) Sr–Nd–Pb isotope data for Fuerteventura (Canary Islands) basal complex and subaerial volcanics: application to magma genesis and evolution. Schweiz Mineral Petrogr Mitt 71:5–21

Hoernle K, Tilton G, Schmincke H-U (1991) Sr–Nd–Pb isotopic evolution of Gran Canaria: evidence for shallow enriched mantle beneath the Canary Islands. Earth Planet Sci Lett 106:44–63

Hoernle K, Zhang Y-S, Graham D (1995) Seismic and geochemical evidence for large- scale mantle upwelling beneath the eastern Atlantic and western and central Europe. Nature 374:34–39

Hoernle K, Werner R, Morgan JP, Garbe-Schönberg D, Bryce J, Mrazek J (2000) Existence of complex spatial zonation in the Galápagos plume for at least 14 m.y. Geology 28:435–438

Holm PM, Wilson JR, Christensen BP, Hansen L, Hansen SL, Hein KH, Mortensen AK, Pedersen R, Plesner S, Runge MK (2006) Sampling the Cape Verde mantle plume: evolution of melt compositions on Santo Antão, Cape Verde Islands. J Petrol 47:145–189

Holm PM, Grandvuinet T, Friis J, Wilson JR, Barker AK, Plesner S (2008) An ^{40}Ar–^{39}Ar study of the Cape Verde hotspot: temporal evolution in a semi-stationary plate environment. J Geophys Res B08201:2007J. doi:10.1029/B005339

Kelemen PB, Hart SR, Bernstein S (1998) Silica enrichment in the continental upper mantle via melt/rock. Earth Planet Sci Lett 164:387–406

Kloeck W, Palme H (1988) Partitioning of siderophile and chalcophile elements between sulfide, olivine, and glass in a naturally reduced basalt from Disko Island, Greenland. In: Ryder G (ed) Proceedings of the Lunar and planetary science conference, vol 18. Pergamon, New York, pp 471–483

Kogiso T, Hirschmann MM, Frost DJ (2003) High-pressure partial melting of garnet pyroxenite: possible mafic lithologies in the source of ocean island basalts. Earth Planet Sci Lett 216:603–617. doi:10.1016/S0012-821X(03)00538-7

Kogiso T, Hirschmann MM, Pertermann M (2004a) High-pressure partial melting of mafic lithologies in the mantle. J Petrol 45:2407–2422. doi:10.1093/petrology/egh057

Kogiso T, Hirschmann MM, Reiners PW (2004b) Length scales of mantle heterogeneities and their relationship to ocean island basalt geochemistry. Geochim Cosmochim Acta 68:345–360

Kokfelt TF, Holm PM, Hawkesworth CJ, Peate DW (1998) A lithospheric mantle source for the Cape Verde Island magmatism: trace element and isotopic evidence from the Island of Fogo. Mineral Mag 62A:801–802

Le Bas MJ (1989) Nephelinitic and basanitic rocks. J Petrol 30:1299–1312

Lundstrom CC, Hoernle K, Gill J (2003) U-series disequilibria in volcanic rocks from the Canary Islands: plume versus lithospheric melting. Geochim Cosmochim Acta 67:4153–4177

Martins S, Mata J, Munhá J, Mendes MH, Maerschalk C, Caldeira R, Mattielli N (2009) Chemical and mineralogical evidence of the occurrence of mantle metasomatism by carbonate-rich melts in an oceanic environment (Santiago Island, Cape Verde). Mineral Petrol. doi:10.1007/s00710-009-0078-x

Millet M-A, Doucelance R, Schiano P, David K, Bosq C (2008) Mantle plume heterogeneity versus shallow-level interactions: a case study, the São Nicolau Island, Cape Verde archipelago. J Volcanol Geotherm Res 176:265–276. doi:10.1016/jjvolgeores.2008.04.003

Montelli R, Nolet G, Dahlen FA, Masters G, Engdahl ER, Hung S-H (2004) Finite-frequency tomography reveals a variety of plumes in the mantle. Science 30:338–343

Montelli R, Nolet G, Dahlen FA, Masters G (2006) A catalogue of deep mantle plumes: new results from finite-frequency tomography. Geochem Geophys Geosyst 7:Q11007. doi:10.1029/2006GC001248

Mourão C, Mata J, Doucelance R, Maderia J, Millet M-A, Moreria M (2012) Geochemical temporal evolution of Brava Island magmatism: constraints on the variability of Cape Verde mantle sources and on carbonatite–silicate magma link. Chem Geol 334:44–61

Neumann ER, Sorensen VB, Simonsen SL, Johnsen K (2000) Gabbroic xenoliths from La Palma, Tenerife and Lanzarote, Canary Islands: evidence for reactions between ma®c alkaline Canary Islands melts and old oceanic crust. J Volcanol Geotherm Res 103:313–342

Ogg JG (1995) Magnetic polarity time scale of the phanerozoic. In: Ahrens TJ (ed) Global earth physics: a handbook of physical constants, vol 1. AGU Ref. Shelf, Washington, DC, pp 240–270

Pertermann M, Hirschmann MM (2002) Trace-element partitioning between vacancy-rich eclogite clinopyroxene and silicate melt. Am Mineral 87:1365–1376

Pim J, Peirce C, Watts AB, Grevemeyer L, Krabbenhoeft A (2008) Crustal structure and origin of the Cape Verde rise. Earth Planet Sci Lett 272:422–428

Prytulak J, Elliott T (2007) TiO_2 enrichment in ocean island basalts. Earth Planet Sci Lett 263:388–403

Regelous M, Hofmann AW, Abouchami W, Galer SJG (2003) Geochemistry of lavas from the Emperor Seamounts, and the geochemical evolution of Hawaiian magmatism from 85 to 42 Ma. J Petrol 44:113–140

Ryabchikov ID, Ntaflos T, Kurat G, Kogarko LN (1995) Glass-bearing xenoliths from Cape Verde: evidence for a hot rising mantle jet. Mineral Petrol 55:217–237

Simonsen SL, Neumann E-R, Seim K (2000) Sr–Nd–Pb isotope and trace-element geochemistry evidence for a young HIMU source and assimilation at Tenerife (Canary Island). J Volcanol Geotherm Res 103:299–312

Sobolev AV, Hofmann AW, Sobolev SV, Nikogosian IK (2005) An olivine-free mantle source of Hawaiian shield basalts. Nature 434:590–597

Sobolev AV, Hofman AW, Kuzmin DV, Yaxley GM, Arndt NT, Chung SL, Danyushevsky LV, Elliott T, Frey FA, Garcia MO, Gurenko AA, Kamenetsky VS, Kerr AC, Krivolutskaya NA, Matvienkov VV, Nikogosian IK, Rochell A, Sigurdsson IA, Sushchevskaya NM, Teklay M (2007) The amount of recycled crust in source of mantle-derived melts. Science. doi:10.1126/science.1138113

Stracke A, Bourdon B (2009) The importance of melt extraction for tracing mantle heterogeneity. Geochim Cosmochim Acta 73:218–238. doi:10.1016/j.gca.2008.10.015

Stracke A, Hofmann AW, Hart SR (2005) FOZO, HIMU, and the rest of the mantle zoo. Geochem Geophys Geosyst 6:Q05007. doi:10.1029/2004GC000824

Thirlwall MF (1997) Pb isotopic and elemental evidence for OIB derivation from young HIMU mantle. Chem Geol 139:51–74

Thirlwall MF, Gee MAM, Taylor RN, Murton BJ (2004) Mantle components in Iceland and adjacent ridges investigated using double-spike Pb isotope ratios. Geochim et Cosmochim Acta 68:361–386

Widom E, Hoernle KA, Shirey SB, Schmincke H-U (1999) Os isotope systematics in the Canary Islands and Madeira: lithospheric contamination and mantle plume signatures. J Petrol 40:297–314

Yaxley GM, Green DH (1998) Reactions between eclogite and peridotite: mantle refertilisation by subduction of oceanic crust. Schweiz Mineral Petrogr Mitt 78:243

Zindler A, Hart S (1986) Chemical geodynamics. Annu Rev Earth Planet Sci 14:493–571